

Concentric Neutral Degradation and Failure Analysis: Sensors and Methods for In-Service Diagnosis

Final Report

Faculty Researchers: Tom Devine, James Evans, Richard White, Paul Wright

Postdoctoral Researchers: Kanna Krishnan, Igor Paprotny

Student Researchers: Giovanni Gonzales, Kristine Jecen, Joe Lemberg, Pierro Marcolongo, Adam Tornheim, Zuoqian (Joe) Wang, Qiliang (Richard) Xu,

POB219-B01

June 30th 2010

Performing Institution Project Managers: [Paul Wright and Igor Paprotny](#)

Commission Project Manager: [Mike Gravely](#)

Abstract: This report describes the final results from the project “Concentric Neutral Degradation and Failure Analysis: Sensors and Methods for In-Service Diagnosis” in which we investigated three on-line techniques for probing the concentric neutrals (CNs) of underground distribution cables. We have shown that both the surface-guided RF wave (Goubau Wave – GW) and the amorphous magnetoresistive (AMR) sensing technique produces a signature that can be used to detect failed CN wires. In the case of the AMR method, we demonstrated the detection of a faulty CN from at least 200 feet away from the location of the break. Similar result was found with respect to the GW method, however the GW is heavily attenuated by the surrounding soil, and hence further experiments have to be conducted to establish its practicality. The two-wire transmission line technique was shorted by the Semicon, and hence no signal was detected over the distance of a typical underground distribution cable.

Introduction

This final report describes the final results from the project “Experimental Methods and Data Analysis of Damaged Concentric Neutrals in Underground Power Distribution Cables” aiming at investigating on-line techniques for probing the concentric neutrals (CNs) of underground distribution cables. As we outline in this report, we have made significant progress in investigating three candidate techniques for on-line CN probing: 1) surface-guided RF waves (Goubau Waves - GW), 2) two-wire RF transmission line, and 3) Amorphous MagnetoResistive (AMR) probing. The results are outlined in the following sections.

1. Surface-guided RF waves (Goubau Waves - GW)

1.1. Introduction:

In this method, we aim to use a surface guided RF-wave called the Goubau Wave (GW) [1,2] to detect breaks in the CNs of underground power distribution cables. The GW is launched along the cable using a conical launching device (funnel) and a non-invasive

capacitive coupling with the CNs, allowing the cable to remain energized while probing is performed. The GW is guided along the cable, and any discontinuities or breaks in the CNs will affect the signal transmitted to a neighboring vault.

1.2. Experimental Setup:

The GW experiments were conducted on three setups: 1) single-wire transmission line (in-lab), 2) elevated underground power distribution cable (in-lab), and 3) partially placed on the ground power distribution cable (outdoors). In all experiments, the RF-signal was generated using an Agilent E8251A programmable signal generator, and modulated with a pulse from an Agilent 33220A arbitrary function generator. A 4-channel 2GHz digital oscilloscope (Agilent Infinium DSO80204B) was used to register both the transmitted and received signals. The power of the received signal was also recorded using the Agilent 8562EC spectrum analyzer.

Setup 1:

Approximately 30 feet of single insulated braided copper wire (\varnothing 4 mm) was suspended one foot below the ceiling to facilitate unobstructed transmission of the GW. A photograph of this setup is shown in Fig. 1.left, while a schematic of the setup is shown on Fig. 1.right. The signal was coupled galvanically at both ends of the wire.

Setup 2:

The signal was capacitively coupled to CNs in a 90 feet section of a 1" 10 CN jacketed TRXLPE cable (ICC Brand-MTT, #2 Solid Al, 175 Mils TRXLPE 15KV, Insulating PF Jacket). The cable was elevated on ten 29-inch tall plastic traffic cones to avoid the interaction of the wave with the reinforced concrete floor underneath. The launching and receiving funnels were made of 5-mil thick soft copper foil, with an outer diameter of 11.5 inches, and an inner diameter of 2 inches. The funnels were attached to 11.5-inch long coaxial sleeves, which were meant to encourage the transition from TEM to TM mode. The cable looped around the room; the transmitting and receiving funnels were separated by approximately 6 feet. A photograph of this setup is shown in Fig. 2



Figure 1. The in-lab single green insulated wire GW setup. **(left)** Photograph showing the wire (i), launch (ii) and receive (iii) cones. **(right)** Schematic of the GW setup.



Figure 2. The 90 foot in-lab underground cable GW setup. The cable was elevated on ten 29 inch tall plastic traffic cones, to avoid the interaction of the wave with the reinforced concrete floor underneath.

Setup 3:

The signal was capacitive coupled to CNs in a 65 feet section of a 1" 10 CN jacketed TRXLPE cable (ICC Brand-MTT, #2 Solid Al, 175 Mils TRXLPE 15KV, Insulating PF Jacket). The cable was partially suspended on 29-inch tall plastic traffic cones. At times, a part of the cable was placed on the ground covered by wood-chips and loose earth, and at times passing through an 11.5-foot long section of an underground PVC duct. The launching and receiving funnels were identical to those in Setup 2. Photographs of this setup are shown in Fig. 3.



Figure 3. The 64 feet outdoor underground cable GW setup. The cable was at times completely (**top-left**) or partially (**top-right, bottom**) supported by 29-inch tall plastic traffic cones.

1.3. Results:

We have successfully demonstrated the ability to launch and couple the GW to a single insulated wire (setup 1). Fig. 4 shows attenuation of a signal transmitted through the cable, displaying behavior that is consistent with good coupling of the GW. Tab. 1 shows the theoretical and measured extend of the field of the GW, showing a very good correspondence between the measured and calculated results.

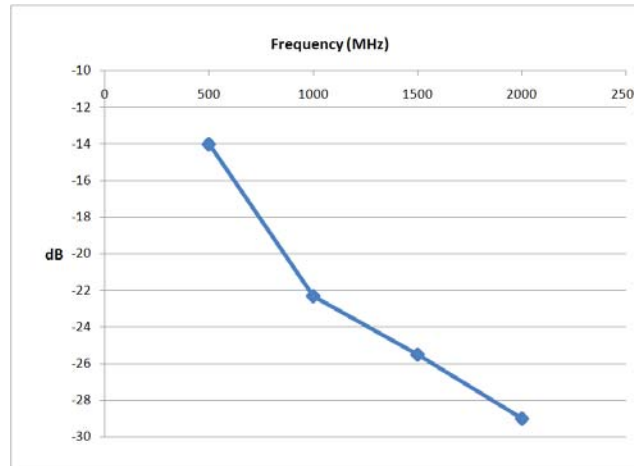


Figure 4. Attenuation of the transmitted signal thorough the cable as a function of frequency, indicating behavior consistent with a transmitted GW.

Table 1. Comparison between theoretical and measured extent of the field for the GW.

Frequency	Theoretical extent (90%)	Observed attenuation at
500 MHz	27 cm	24 cm
2 GHz	8.4 cm	7 cm

We have successfully demonstrated the ability to launch and couple the GW on the CNs of an underground power distribution cable (setup 2). The optimum carrier frequency is lower than in the case of the single conductor wire. Fig. 5.left shows attenuation of a frequency swept of the carrier signal (galvanically coupled to the CNs), using a 14 dBm transmitting signal, indicating an optimum carrier frequency of approximately 300 MHz. Fig. 5.right shows the time-domain (TD) plot of the received signal, modulated with a 200 ns rectangular pulse.

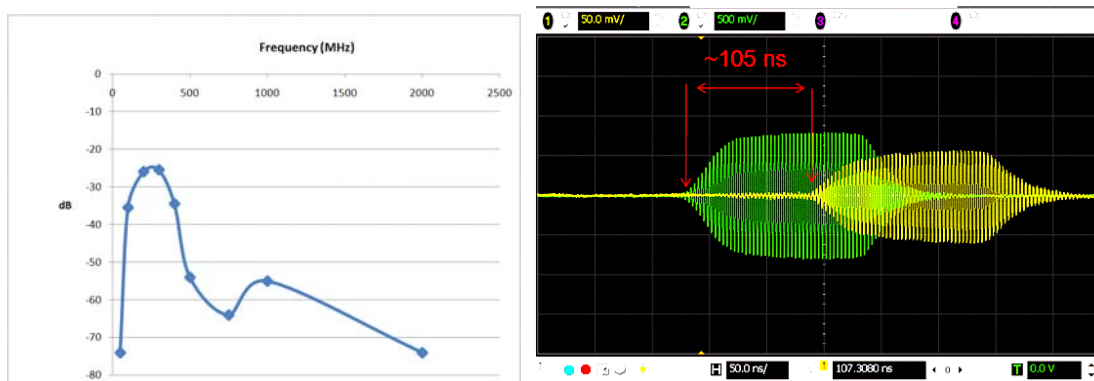


Figure 5. Results indicating successful launch and coupling of the GW to an underground power cable (setup 2). **(left)** Attenuation of swept frequency using a 14 dBm carrier signal, indicating 300 MHz as the optimal GW carrier frequency. **(right)** Screen capture from the DSO80204B oscilloscope showing the time-domain analysis of the superimposed transmitted (yellow) and received (green) 300 MHz 14 dBm signal modulated with a 200 ns rectangular pulse. The observed time delay of approximately 105 ns between the transmitted and received signal correspond to a relative velocity of

propagation (VOP) of 86%, indicating the majority of the energy travels in air surrounding the cable, as expected.

We also showed that the GW could be launched without a galvanic contact with the CN. Fig. 6 shows the TD-plot of a GW signal coupled to the CN using a capacitive coupling at both the receive and transmit funnels. The signal-carrying central conductor from the coaxial cable was connected with a 4.5 inch wide copper sleeve wrapped around the cable jacket. The measured insertion loss associated with the capacitive coupling was approximately 1-2 dB.

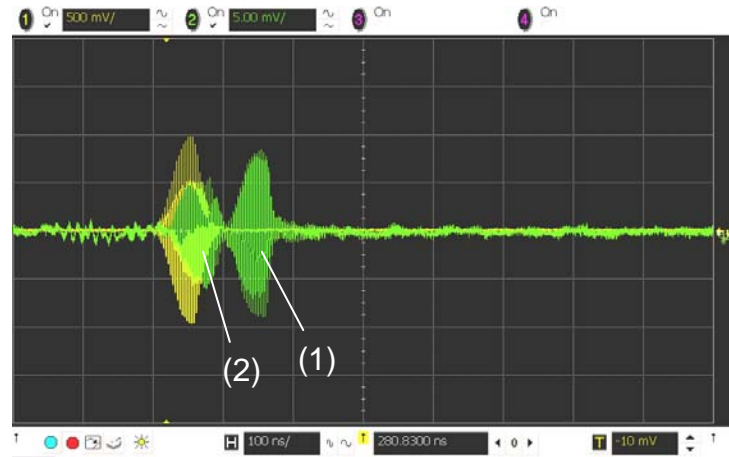


Figure 6. Screen capture from the DSO80204B oscilloscope showing the time-domain analysis of the superimposed transmitted (yellow) and received (green) 300 MHz 14 dBm signal modulated with a 80 ns rectangular pulse, transmitted through the capacitively coupled cable. A ≈ 100 ns delayed transmitted pulse (1 - green) is clearly visible, however part of the signal is now transmitted through radiation, as it is indicated by the short time of the receipt of pulse (2).

As expected, the characteristic of the transmitted signal is changed as it passes over a defect in the CNs. Fig. 7 left and right shows the transmitted (1) and radiated (2) pulses before and after a 5-inch gap was cut in all the CNs, respectively. The cut was made approximately 20 feet from the receiving funnel. An increase in the amplitude of the radiated pulse (2), and a decrease in the amplitude of the transmitted pulse (1) can clearly be seen. This indicated that some of the power is now radiated away at the CN break. Figs. 8 left and right show a 100 ns GW pulse transmitted through a 5-inch and a 60-inch gap, respectively, cut through all the CNs. Again, clearly visible is the decrease in size of the transmitted pulse (1), and the increase in size of the radiated pulse (2).

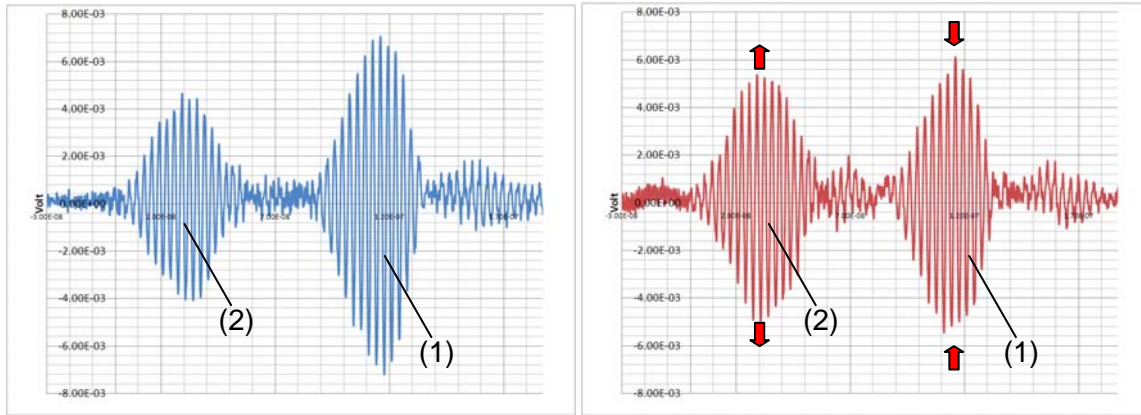


Figure 7. Change in the transmitted GW pulse due to a 5 inch cut in all the CNs. **(left)** The transmitted (1) and radiated (2) pulses (80 ns modulation) prior to the cut. **(right)** The transmitted (1) and radiated (2) pulses (80 ns modulation) after a 5 inch cut was made in all the CNs. Red arrows indicate the relative change in the energy of the peaks, indicating that the power is *radiating* away from the cut.

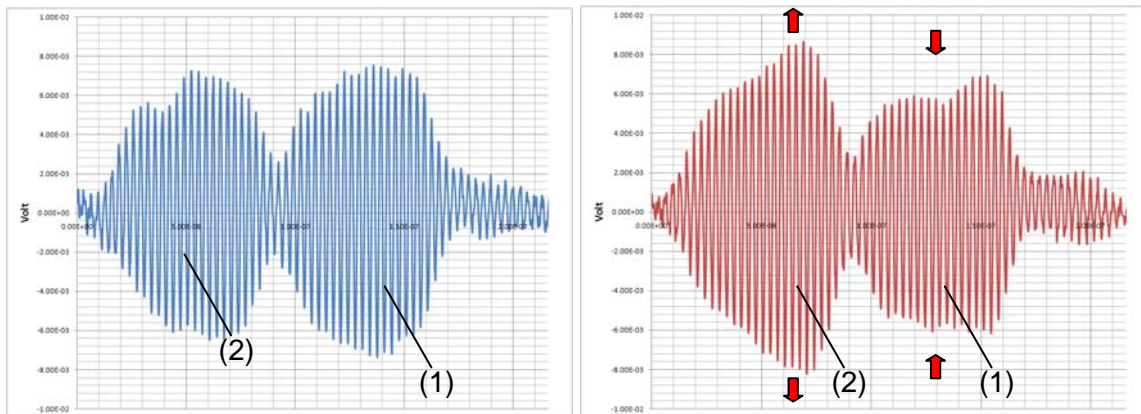


Figure 8. Change in the transmitted GW pulse when the CN cut is enlarged from 5 to 60 inches. **(left)** The transmitted (1) and radiated (2) pulses (100 ns modulation) after a 5 inch cut was made in all the CNs. **(right)** The transmitted (1) and radiated (2) pulses (100 ns modulation) after the cut was enlarged to 60 inches. Red arrows indicate the relative change in the energy of the peaks, indicating that the power is radiating more from the longer cut.

Both these results indicate a significant *relative* change in the characteristics of the transmitted signal, indicating that the detection of sections of damaged CNs should be feasible. However, more modeling and analysis of the transmitted signal is necessary to establish an absolute metric, i.e., a signal characteristic which indicates broken CNs on a cable with no prior GW data. Because the RF signal is emanating from the cable at the point of the break, it may be possible to localize the defect using the emanating RF signal from the surface.

Because the GW is simply guided by the CNs and travels mostly in the space surrounding the cable, experiments were performed to establish the ability of the GW to penetrate soil surrounding the underground cable (Setup 3). For simplicity, the cable was simply placed on the ground, causing only half of the wave to pass through soil. We assume that this allows us to place an upper bound on the transmission of the GW through this kind of soil.

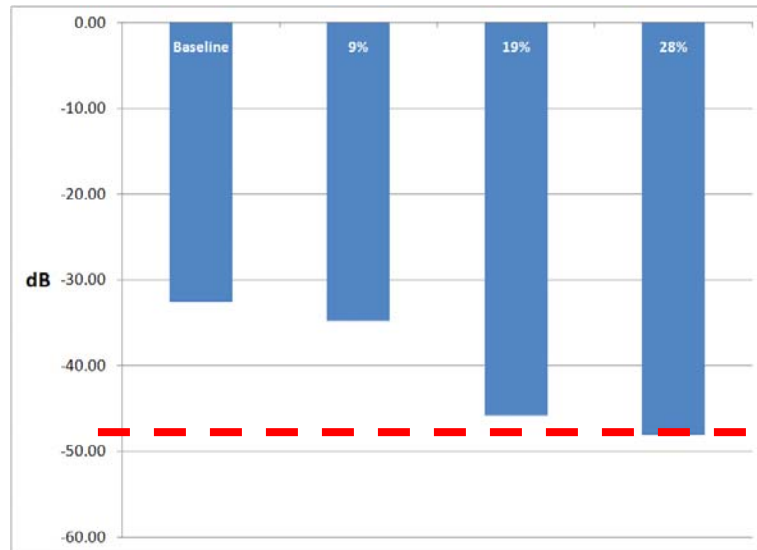


Figure 9. Attenuation of the GW using 300MHz carrier frequency as it passes through the 64 feet underground power distribution cable as its sections are progressively being lowered onto the ground. The data is annotated with the percentage of the cable resting on the ground, the baseline corresponds to the cable entirely elevated (0 %). The red line indicates the noise-floor of the received signal. At 19%, the signal is difficult to discern, and at 28% the signal drops below the noise-floor. (28% corresponds to about 18 ft of cable).

The results of this experiment are summarized in Fig. 9. The signal deteriorated rapidly below the noise floor, and was undetectable after 18 ft (28%) of the cable was placed on the ground, and a similar result was observed when the cable was passing through a 11.5 feet long PVC duct. This result may seem discouraging, but note that this setup suffered from very high insertion loss, most likely due to impedance mismatch between the coaxial cable and the GW transmission line; this is clearly indicated by the 32 dB loss in the baseline signal. This illustrates the need to re-design the GW couplers to reduce the insertion loss.

In addition, a frequency scan of the entire cable placed on the ground (see Fig. 10) showed a significant and appropriately time-delayed peak at 400 MHz, as shown in Fig. 11. This may indicate a shift of the optimal coupling frequency for the GW from 300 MHz when passing through soil. This was not collaborated by a frequency scan when the cable was passed through the PVC duck, but the scan was taken at 100 MHz intervals, and a sharp peak in the transmitted signal could have been missed.



Figure 10. The setup for a frequency scan with the cable completely placed on the ground, with the exception of the sections around the sending and the receiving funnels, which have to be elevated to avoid deforming the funnel geometry.

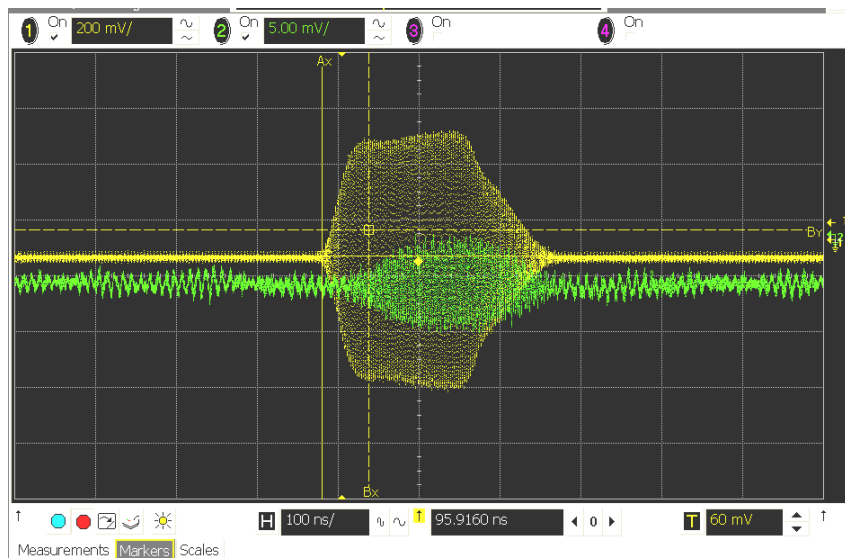


Figure 11. A GW pulse transmitted through setup in Fig. 10 using a carrier frequency of 400 MHz. The attenuation was on average 39 dB, about 7 dB above the noise floor. The pulse was delayed by approximately 77 ns, indicating the signal traveled along the entire cable.

1.4. Conclusions:

We have analyzed the GW mode of propagation, and constructed conical launching devices that allow us to successfully couple the GW to underground power distribution cables. We have artificially induced breaks in the CNs, and have shown that such breaks cause a significant change in the transmitted signal. As the majority of the energy of the GW is situated outside the cable, we see a fair amount of attenuation in the transmitted signal as the wave is passing through surrounding soil. Additional modeling and experiments need to be performed to establish the minimum attenuation of the signal due to surrounding soil.

For instance, the apparent shift from 300 MHz coupling frequency should be further investigated.

Future work should encompass modeling of the GW propagation along the underground power distribution cable surrounded by soil, re-design of the launching/receiving funnels to minimize impedance mismatch and increase coupling efficiency, use higher than 14dBm transmission power, and perform a denser frequency/group delay scan. These tests should help to decide the practicality of this CN probing method. The potential of using RF signals radiating from the breaks in the CNs as means of localizing them should also be investigated.

2. Two-wire Transmission Lines

2.1. Introduction:

A two-wire transmission line carries at one instant a forward load current in one conductor and a return current in the opposite direction. The two lines have a distributed series impedance consisting of resistance R and inductance L per unit length and distributed parallel admittance consisting of conductance G and capacitance C per unit length. The transmission line has a characteristic impedance Z , angular frequency ω and velocity of propagation v dependent on the above four parameters. Typically R and G are very small as compared to the impedances $j\omega L$ and $1/j\omega C$. For the two-wire transmission line with wires of diameter a separated by distance d , the expressions for L and C are given by equations (1-3) [1]:

$$\frac{\varepsilon}{C} = \frac{L}{\mu} = \cosh^{-1}\left(\frac{a}{d}\right) \quad (1)$$

$$Z = \sqrt{\frac{\mu}{\varepsilon}} \quad (2)$$

$$v = \sqrt{\frac{1}{\mu\varepsilon}} \quad (3)$$

The CNs are in conductive contact with the Semicon layer beneath them. The typical conductivity of Semicon is about 1 Siemens/meter and the capacitance is about 300 pF/meter, resulting in a typical time-constant $\varepsilon/\tau = 300$ ps. This value is for an intact cable with CNs making good contact with the Semicon over the length of the cable. If the Semicon layer separates from one of the CNs over a significant length, which is to be determined experimentally, the resistance between the two increases along with the time-constant τ . This may enable detecting a reflected pulse using two-wire Time Domain Reflectometry (TDR) and approximating the location of the CN-Semicon separation.

2.2. Initial Experimental Results:

A pilot study was performed to test the effectiveness and coupling of a RF-signal to the two-wire transmission line consisting of two adjacent CNs. This was test by driving a sine

wave of amplitude 20 V peak-to-peak with frequency from 1 MHz to 20 MHz and the output measured at the other end of a 3-foot, 5-inch cable galvanically connected to the copper CNs. A reference measurement is made with galvanic coupling at both ends for comparison. The setup for the experiments is shown in Fig. 12.left, while the experimental results are presented in Fig. 12.right. As can be seen for the results in Fig. 12.right, the RF-signal is shorted by the Semicon, resulting in high attenuation, even across the 3-foot, 5-inch cable section. We observed no signal across the 200-foot section; this is not surprising, as the measured impedance between adjacent CNs was 1-2 ohms.

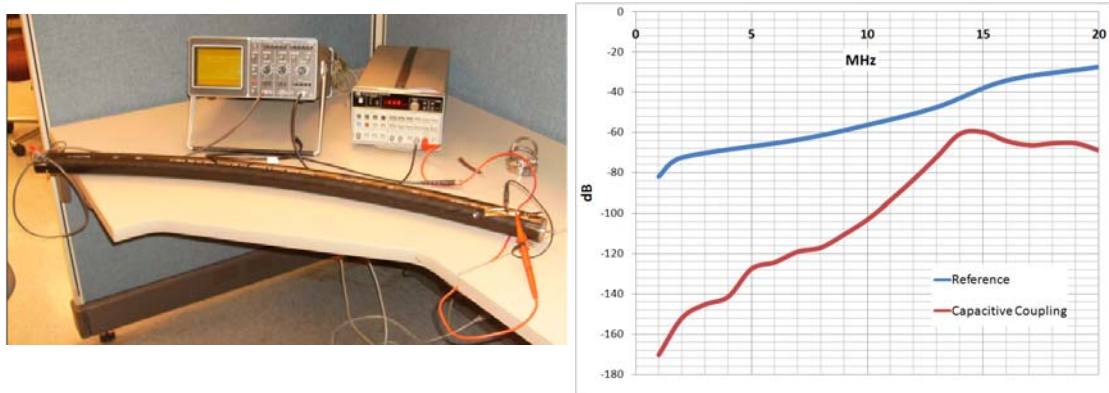


Figure 12. Pilot study of the 2-wire transmission line using adjacent CNs. **left:** Experimental setup using a 3-foot, 5-inch underground power distribution cable section. **right:** Results from the experiments showing high attenuation of the signal due to the shortening effect of the Semicon.

2.3. Conclusions:

Although a weak signal can be transmitted through a 2-wire transmission line composed of adjacent CNs on short cable lengths, over longer distances the Semicon shorts the RF-signal preventing the waveform from traveling to the other side of the cable. We conclude that the 2-wire transmission line is not a practical CN probing method.

3. Amorphous Magnetoresistive (AMR) CN Sensing

3.1. Introduction:

We investigated a method for diagnosing the health of CNs in underground power distribution cables using a 3-axis magnetic field sensor placed in close proximity or contact with the outside of the cable, and either moved along the cable in the axial direction, or rotated around the jacketed cable [3]. From this magnetic field information the currents in the individual concentric neutrals can be determined with enough accuracy to detect asymmetries due to faulty concentric neutrals. We use the Amorphous MagnetoResistive (AMR) effect of a commercial sensor (Honeywell - HMC1043) due to its high sensitivity. The AMR effect is a physical phenomenon whereby certain thin-film structures vary their electrical resistance depending on the magnetic flux passing through them [4].

3.2. Modeling:

The magnetic fields outside of a cable due to currents in the center conductor and CNs were modeled using a simplified two-dimensional model implemented in MATLAB. In this model, the CNs were treated as straight wires distributed evenly around the center conductor of a two-inch diameter cable containing twelve concentric neutrals. Calculations of the magnetic field at the simulated sensor location were carried out by use of the Biot-Savart law. To simulate the axial movement of the sensor, which occurs during experiments, the sensor was modeled to rotate around the circumference of the two-dimensional model. In all simulations, the total current carried by the CNs was set to be $3A_{RMS}$.

Modeling indicated that a faulty CN creates a perturbation that is detectable in all three magnetic axes (see Fig. 13). Our modeling also indicated that a CN break should be detectable from up to several hundred feet from the breakpoint.

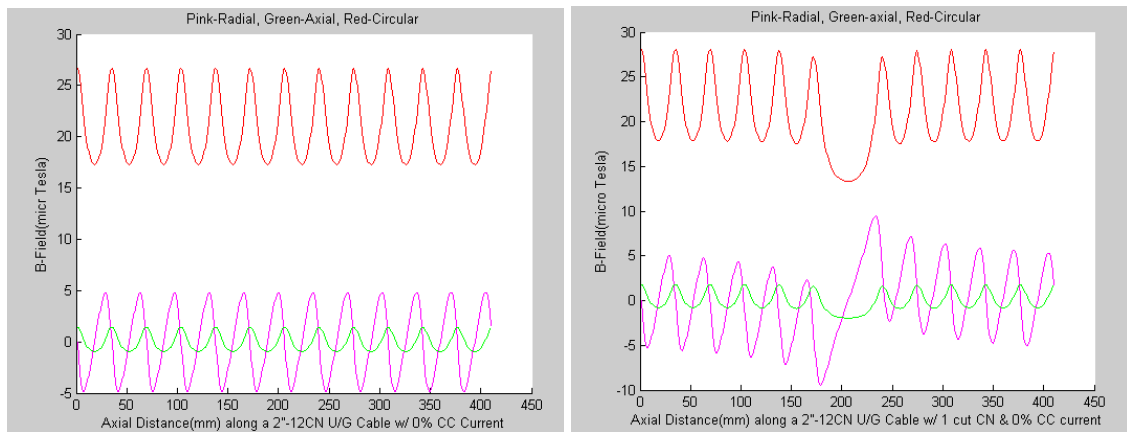


Figure 13. Results from modeling of the magnetic field around an underground distribution cable with total of $3 A_{RMS}$ passing through the CNs. The symmetric pattern of the magnetic field in a healthy cable (left) is perturbed by a faulty CN wire (right). The results here were for clarity taken with no current flowing through central conductor.

3.3. Experimental Setup:

The experiments were performed on a section of two-inch diameter, jacketed, XLPE-insulated cable. Two variable transformers driven by 60Hz line voltage were used to drive currents in the central conductor and concentric neutrals, respectively. In each experiment, $3A_{RMS}$ was driven through all the CNs connected in parallel, and a fraction of the current was driven through the center conductor. A one-ohm current-balancing load resistor was placed in series with each concentric neutral at the termination of the cable to ensure an even distribution of current among the unbroken concentric neutrals.

The same length of cable was used for those experiments in which a concentric neutral was treated as broken. To simulate this break, one of the one-ohm balancing resistors was removed from the circuit, leaving the corresponding concentric neutral carrying zero current.

The amorphous magnetoresistive (AMR) sensor used is the HMC1043 device, manufactured by Honeywell. This device is three millimeters square, and thus possesses good spatial resolution to distinguish between the currents in separate concentric neutrals. The device was provided by Honeywell soldered to a one inch square PCB with onboard amplifier. The device was powered by an Agilent E3631A DC power supply. Because the AMR device needs periodic set/reset pulses to function correctly, an Agilent 33220A function generator was used to provide a set/reset pulse to the device every four minutes. The AMR sensor was passed down the axial length of the cable and the three-axis values of magnetic field on the surface of the cable jacket were recorded. The total length of travel was slightly larger than that required to pass above one concentric neutral twice. The AMR sensor was moved with a metric lead screw assembly for this experiment, but consideration has been given to deployable measurement techniques.

3.4. Results:

Figs. 14 - 17 depict the three axes of magnetic field outside the experimental cable for one ratio of current (center conductor to concentric neutral) and one condition of the experimental concentric neutral (broken or unbroken). Note that the magnetic field values are RMS values, yet they swing positively and negatively; our convention is to plot the magnitude of the RMS value as positive or negative to indicate the phase of the 60Hz B-field waveform at that point as referenced against the line voltage. Thus, these curves indicate the phase of the magnetic field waveform as well as RMS magnitude of the magnetic field.

Apparent in the curves is a series of peaks, each corresponding to sensor located directly above a current-carrying concentric neutral. In the two sets of curves for which a concentric neutral was broken, a characteristic disturbance can be seen: in the axial and circumferential fields this disturbance appears as a local minimum where a current peak would appear in a healthy cable, as predicted by modeling. In the radial field, this disturbance appears as a swing between phases and between two peaks, similarly to that predicted by modeling.

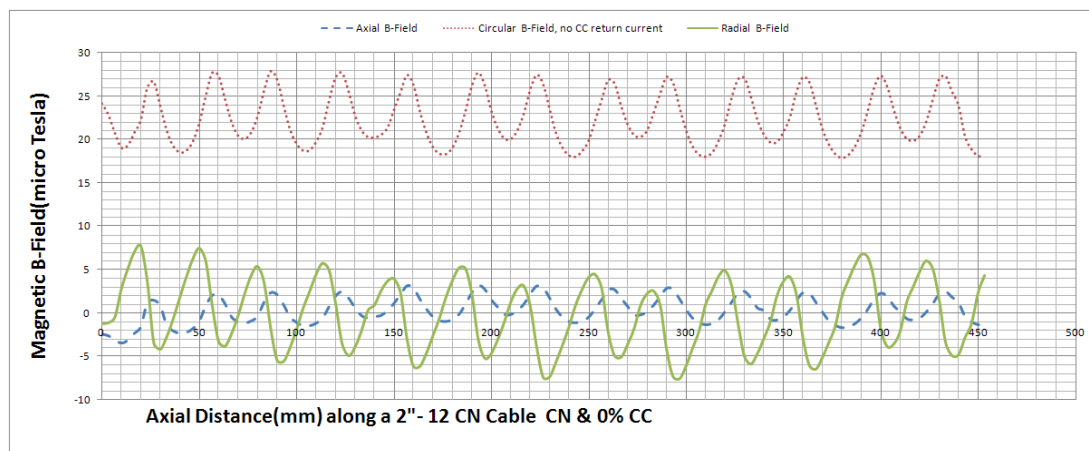


Figure 14. 0% center conductor (CC) current.

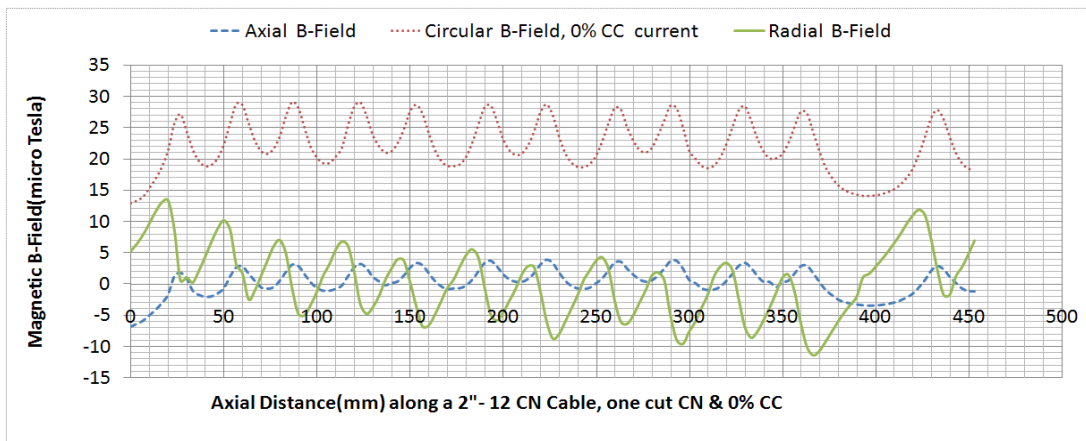


Figure 15. 0% center conductor (CC) current, one broken concentric neutral (CN)

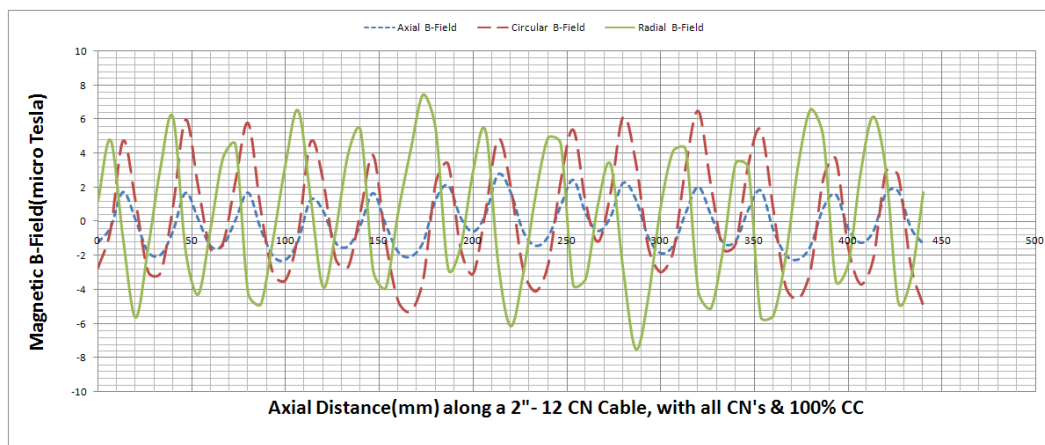


Figure 16. 100% center conductor (CC) current.

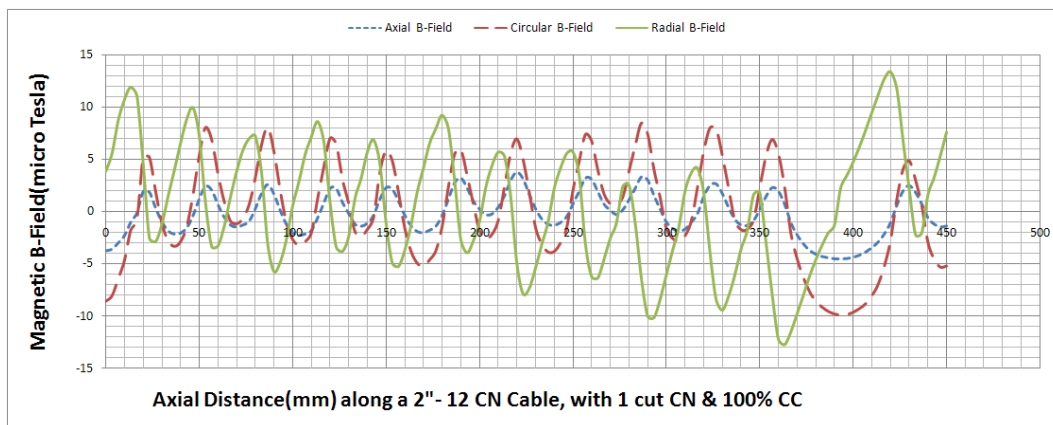


Figure 17. 100% center conductor (CC) current, one broken concentric neutral (CN).

In order to provide the user with a more quantitative way of locating CN-failure, we investigated using a Fast-Fourier Transform (FFT) as a way of identifying faulty cables. The FFT allows us to clearly identify the segment of cables where one or more CNs are

damaged. As shown in Fig. 18, the peaks in the magnetic field around a healthy cable are distributed according to the angular frequency corresponding to the number of CNs. This periodicity is broken if a CN wire stops to conduct current, resulting in a peak around a lower spatial frequency.

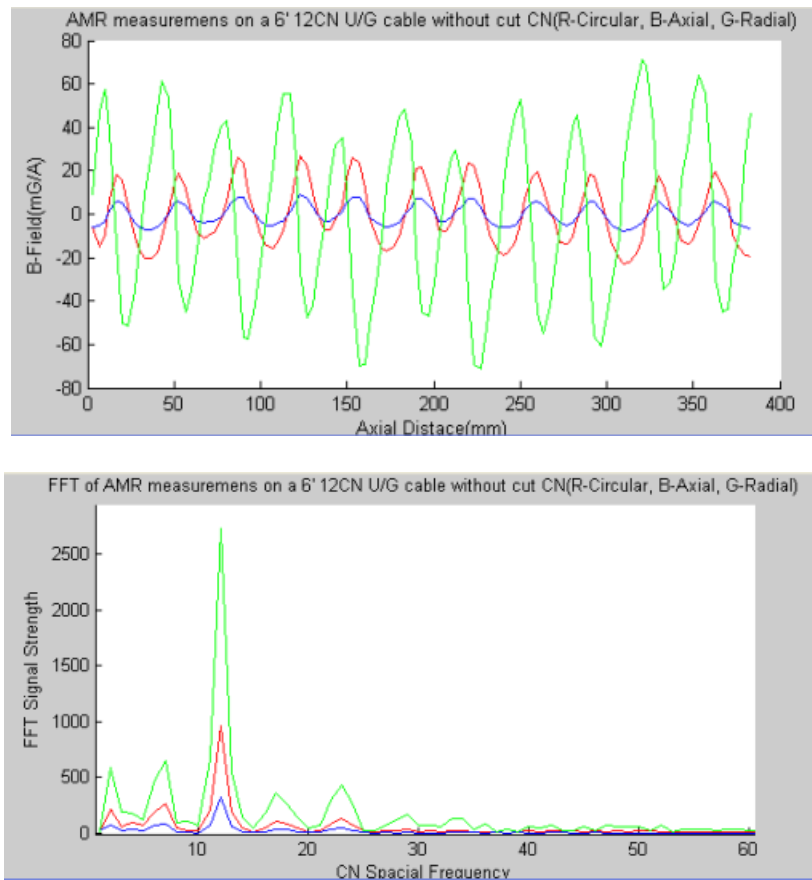


Figure 18. AMR measurements (**top**) and corresponding FFT plot (**bottom**) of a healthy 6-foot cable with 12 CNs, indicating the main FFT peak at #12.

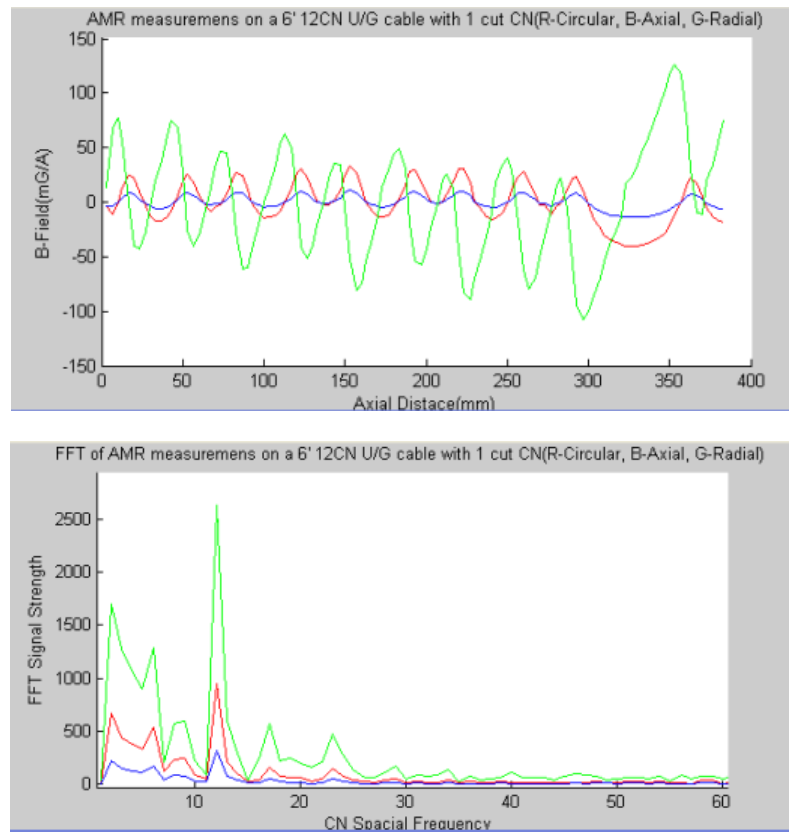


Figure 19. AMR measurements (**top**) and corresponding FFT plot (**bottom**) of a 6-foot cable with 12 CNs, where one of the CNs has been cut. In addition to the main peak at #12, a significant peak is present at low spatial frequency.

Finally, we have experimentally confirmed that we can detect a broken CN from a distance of at least 200 feet, confirming our previously modeled results.

3.5. Conclusions:

We have shown that sensing currents in CNs using AMR magnetic sensors is a promising method for on-line probing of the integrity of CNs in underground power distribution cables. Our modeling has shown that a failed CN can be detected by measuring the magnetic perturbation that affects all three axes of the magnetic field surrounding an energized underground cable, and that such failure can be detected several hundred feet away from the failure point. Our experiments have confirmed the modeling; we have demonstrated that the perturbation affects all three magnetic axes and is detectable at least 200 feet away from the failure site. We have also developed an FFT technique that allows us to rapidly identify the signature of a failed concentric neutral.

Future work should encompass the integration of an in-field deployable experimental setup, which includes wireless communication from the sensor to a data-collecting unit. In addition, one should investigate the behavior of the AMR sensors next to a strong magnetic field emanating from the a current-carrying central conductor, and the reliability of the methods in the presence of typical CN return currents present in the field.

Conclusions

Through the course of this project, we have investigated three candidate techniques for on-line CN probing: 1) surface-guided RF waves (Goubau Waves - GW), 2) two-wire RF transmission lines, and 3) Amorphous MagnetoResistive (AMR) probing. We discovered that both the GW and the AMR probing show a change in the sensory response that can be attributed to damaged concentric neutrals (CNs), albeit the most significant change was observed in the AMR probing method. We found that the two-wire transmission line method is shorted by the Semicon layer, preventing the signal from propagating through the underground cable. At this stage, the AMR method seems the most promising, as we were able to detect the break in the CNs at least 200 feet from the fault location. The GW is heavily attenuated by the soil surrounding the cable, and in most experiments the signal was reduced to the noise-floor after about 20 feet. However a possible observed shift in the preferred GW carrier frequency, allowing us to transmit a clear signal to at least 64 feet, warranting further study.

Additional research needs to be performed on both the GW and AMR methods to determine their practicality for on-line CN probing. In particular, the effects of soil, as well as utilizing the GW at a higher power should be investigated. With respect to the AMR, it is important to study our ability to detect irregularities in the magnetic fields using the actual CN return currents found in the field. We believe the long-term goal should be to incorporate the most practical diagnostic techniques into a self-powered sensor module [5] that would be installed onto legacy or new equipment to provide continues performance monitoring and provide Prognostic Health Management (PHM) of the evolving power grid.

Acknowledgments

The authors would like to thank Walter Zenger, Tony Nothelfer and Al Valenzuela from PG&E, as well as John Erikson from Sempra Energy for providing us with many feet of underground distribution cable, terminations, and test equipment. We would also like to thank our Technical Advisory Committee, as well as Jamie Patterson and Mike Gravely from the California Energy Commission (CEC), for their insightful comments and suggestions.

References

- [1] Goubau, G. "Surface Waves and Their Applications to Transmission Lines," J. App. Phys., Vol. 21, 1950.
- [2] Paprotny, I., R. M. White and K. Krishnan. "RF Transmission-line Methods for In-service Probing of Concentric Neutral Wires in Underground Power Distribution Cables" in the ISEI 2010, June 6-9 2010, San Diego, CA.
- [3] Seidel, M., I. Paprotny, R. M. White and K. Krishnan. "AMR Current Sensors for Evaluating the Integrity of Concentric Neutrals in In-Service Underground Power Distribution Cables" ISEI 2010, June 6-9 2010, San Diego, CA.

[4] Lenz J. and Edelstein A. "Magnetic Sensors and Their Applications." IEEE Sensors, vol. 6, 2006, pp. 631-649.

[5] Paprotny, I., E. S. Leland, C. Sherman, R. M. White and P. K. Wright. Self-powered MEMS Sensor Module for Measuring Electrical Quantities in Residential, Commercial, Distribution and Transmission Power Systems, ECCE 2010, September 12-16 2010, Atlanta, GA.

RF Transmission-line Methods for In-service Probing of Concentric Neutral Wires in Underground Power Distribution Cables

Igor Paprotny

Berkeley Sensor & Actuator Center
University of California
Berkeley, CA, 94720, USA
igorpapa@eecs.berkeley.edu

Richard M. White

Berkeley Sensor & Actuator Center
University of California
Berkeley, CA, 94720, USA
rwhite@eecs.berkeley.edu

Kanna Krishnan

Berkeley Sensor & Actuator Center
University of California
Berkeley, CA, 94720, USA
kannak@berkeley.edu

Abstract— Failure of concentric neutral (CN) wires in an underground power distribution cable can drastically reduce its useful life. New on-line approaches are needed to assess the deterioration of the CNs and to prevent unscheduled service disruptions. In this paper, we present new methods for probing the integrity of CN wires in underground power distribution cables using RF-waves. The primary advantage of our techniques compared to traditional CN diagnostics is the ease of applying our methods to *energized* underground power distribution cables. This paper briefly describes two methods for transmitting RF-waves through underground cables: a surface RF-wave, also called the Goubau Wave (GW), guided by all the CNs within the cable, and an RF-wave coupled to a two-wire transmission line composed of adjacent CNs. We focus on the use of GW to probe for CN degradation, due to good coupling of the wave to the underground cable. We show experimental results demonstrating the change in the signature of the transmitted GW signal through a section of degraded (broken) CNs.

Keywords: *underground cable diagnostics, RF probing methods, Goubau waves, concentric neutrals*

I. INTRODUCTION

Concentric neutral (CN) degradation is a significant failure mechanism for underground distribution cables. It causes loss of protective shielding as well as lack of properly grounded current return path. Existing cable diagnostic techniques, such as TDR require the cable to be disconnected from the grid, causing service disruptions during the testing operation.

In this paper, we present novel methods for testing the integrity of the CNs in an underground power distribution cable without de-energizing it in order to perform the measurement. Our methods use RF signals *coupled* to in-service cables via capacitive couplings at cable endpoints (in underground distribution vaults.) We describe two methods for transmitting RF-waves through these cables: a surface RF-wave, also called the Goubau Wave (GW), guided by all the CNs within the cable, and an RF-wave coupled to a two-wire transmission line composed of adjacent CNs.

In the first method, the GW is launched along the cable using a conical launching device (funnel) and a non-invasive capacitive coupling to the CNs. The GW is then guided along the cable, and any discontinuities, breaks, or corrosion in the CNs will reflect and attenuate the signal transmitted to a neighboring vault.

In the second method, a pair of adjacent CNs is treated as a 2-wire transmission line with distributed R,C,L and G parameters over the length of the cable with a typical characteristic impedance Z_0 . A short voltage pulse applied through a non invasive capacitive coupling to the CNs, can be used to excite the two-wire transmission line. Any cable impairment such as open breaks, short circuits, localized corrosion or other defects will result in reflections of the transmitted signal.

II. TYPICAL UNDERGROUND DISTRIBUTION CABLE

The structure of a typical underground distribution cable is shown on Fig. 1. The cable consists of a central conductor, made out of aluminum or copper (1), and covered with an inner layer of a semiconductive polymer called semicon (2). The semicon layer is encased in an insulated material (3) (such as PE). The insulator is covered with an outer layer of semicon (4). A set of spiraling CNs (5) are places on top of the outer semicon layer. Newer cables contain an outer jacket extruded over the CNs (6).

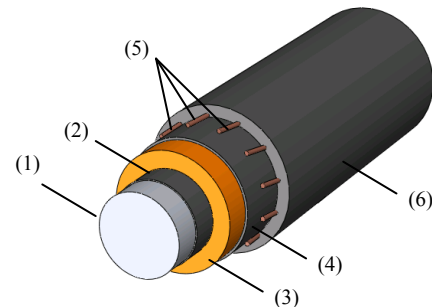


Fig. 1. A typical underground power distribution cable.

III. RF-TRANSMISSION LINES

A. Surface-guided RF Waves (Goubau)

The initial idea of coupling an RF-wave to a conductor with dielectric coating was originally proposed by George Goubau [1]. The wave is guided by the conductor, and its energy is confined in the space around the wire. The dielectric coating restricts the extent of the field. The coupling of the RF signal from a feed coaxial cable (TEM-mode) to the surface-guided mode (TM-mode) is performed using conical launching devices (funnels), such as shown in Fig. 2a (from [2]). The idea is to couple the Goubau Wave (GW) to the concentric neutrals of an underground distribution cable in vault A, perform time-domain reflectometry (TDR) on the returned signal, and perhaps also detect the transmitted signal to vault B (as outlined in Fig. 2b).

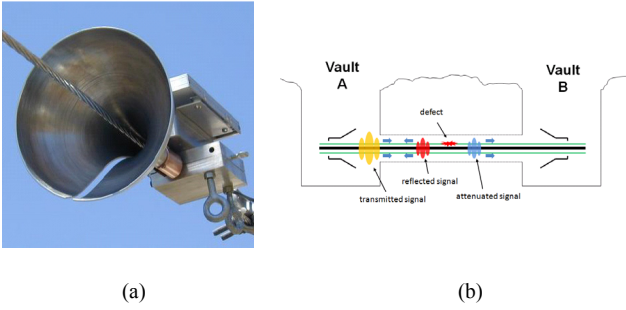


Fig. 2. a: (from [2]) Conical launching device used in a commercial application to couple surface-guided RF waves to overhead power distribution lines. b: Outline of our concept for using the GW for probing underground distribution cables. The probing wave is launched from vault A, attenuation of the transmitted wave is measured in vault B, and TDR is performed on the reflected signal at vault B.

B. Two-wire Transmission Lines

A two-wire transmission line carries at one instant a forward load current in one conductor and a return current in the opposite direction. The two lines have distributed series impedance consisting of resistance R and inductance L per unit length and distributed parallel admittance consisting of conductance G and capacitance C per unit length. The transmission line has a characteristic impedance Z , angular frequency ω and velocity of propagation v dependent on the above four parameters. Typically R and G are very small as compared to the impedances $j\omega L$ and $1/j\omega C$. For the two-wire transmission line with wires of diameter a separated by distance d , the expressions for L and C are given by equations (1-3) [3]:

$$\frac{\epsilon}{C} = \frac{L}{\mu} = \cosh^{-1}\left(\frac{a}{d}\right) \quad (1)$$

$$Z = \sqrt{\frac{\mu}{\epsilon}} \quad (2)$$

$$v = \sqrt{\frac{1}{\mu\epsilon}} \quad (3)$$

The CNs are in galvanic contact with the semicon layer beneath them. The typical conductivity of semicon is about 1 Siemens/meter and the capacitance is about 300 pF/meter, resulting in a typical time-constant $\epsilon/\tau = 300$ ps (assuming an intact cable with CNs making good contact with the semicon over its length). If the semicon layer separates from one of the CNs over a significant length, which is to be determined experimentally, the resistance between the two increases along with the time-constant τ . This enables detecting a reflected pulse using two-wire Time Domain Reflectometry (TDR) and approximating the location of the CN-semicon separation.

IV. EXPERIMENTAL SETUP (GOUBAU)

We now describe the experiments conducted on coupling the GW to an underground power distribution cable. All experiments have been conducted using a 90 feet section of a 1" 10 CN jacketed TRXLPE cable (ICC Brand-MTT, #2 Solid Al, 175 Mils TRXLPE 15KV, Insulating PF Jacket). The launching and receiving funnels were made out of 5 mils thick soft copper foil, with an outer diameter of 11.5 inches, and an inner diameter of 2 inches. The funnels were attached to 11.5 inch long coaxial sleeves, which were meant to encourage the transition from TEM to TM mode. The RF-signal was generated using an Agilent E8251A programmable signal generator, and modulated with a pulse from an Agilent 33220A arbitrary function generator. A 4-channel 2GHz digital oscilloscope (Agilent Infinium DSO80204B) was used to register both the transmitted and received signals. The power of the received signal was also recorded using the Agilent 8562EC spectrum analyzer. The cable was elevated on ten 29 inch tall plastic traffic cones, to avoid the interaction of the wave with the reinforced concrete floor underneath. The cable looped around the room; the transmitting and receiving funnels are separated by approximately 6 feet.

V. EXPERIMENTAL RESULTS (GOUBAU)

A. Galvanic Coupling to the CNs

Initial experiments were conducted to determine our ability to couple the GW to the CNs of a power distribution cable. In this setup, the central conductor of a signal-carrying coaxial cable was galvanically connected to all the CNs (via a hole in the sleeves), while its shield was galvanically connected to the sleeve. Fig. 3 shows the receive power versus frequency for an applied 14 dBm signal, indicating an optimal coupling frequency of around 300 MHz. A screen capture from the DSO80204B oscilloscope showing the time domain analysis of the superimposed transmitted (yellow) and received (green) 300 MHz 14 dBm signal modulated with a 90 ns square pulse is shown on Fig. 4, indicating a clear delay as the pulse follows the entire length of the cable.

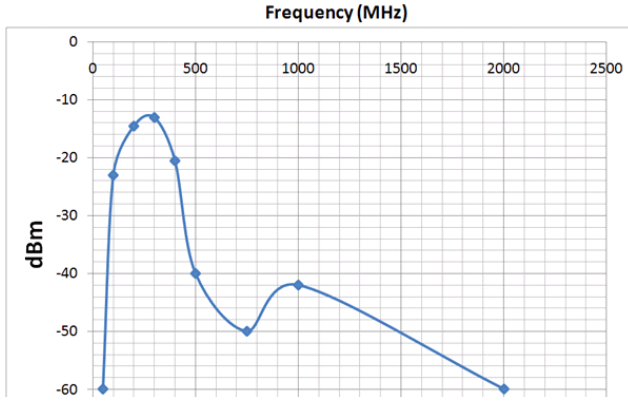


Fig. 3. The receive power (measured at the receiving funnel) versus frequency plot for an applied 14 dBm signal (at the transmitting funnel).

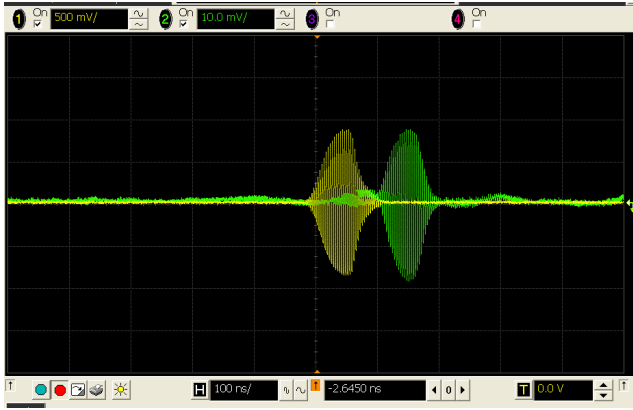


Fig. 4. Screen capture from the DSO80204B oscilloscope showing the time domain analysis of the superimposed transmitted (yellow) and received (green) 300 MHz 14 dBm signal modulated with a 90 ns square pulse. A ≈ 100 ns delay can be seen, indicating that the pulse follows the entire length of the cable.

B. Capacitive Coupling to the CNs

In order for us to use the GW to perform *on-line* diagnosis of *energized* power distribution cables, it is desired to couple the signal without making galvanic contact with the CNs. To achieve this, we installed a capacitive coupling to the CNs at both the receiving and transmitting funnels. The signal-carrying central conductor from the coaxial cable was connected with a 4.5 inch wide copper sleeve wrapped around the cable jacket. Both capacitive couplings were located within the sleeves of the funnels. The insertion loss associated with the capacitive coupling was measured to approximately 1-2 dB, and 300 MHz was determined to be the optimal frequency for the capacitive coupled GW.

However, time domain analysis shows that part of the signal is now transmitted through free-space radiation, increasing the effective insertion loss of the coupling. Fig. 5 shows a screen capture from the DSO80204B oscilloscope of the time domain analysis of the superimposed transmitted

(yellow) and received (green) 300 MHz 14 dBm signal modulated with the 80 ns square pulse and transmitted through the capacitive couplings at the transmit and receive funnels. A ≈ 100 ns delayed pulse (1) is clearly visible, however part of the signal is transmitted through radiation, as it is indicated by a radiated pulse (2). The radiated signal is very susceptible to noise in the environment around both funnels, and exhibits a great deal of variability.

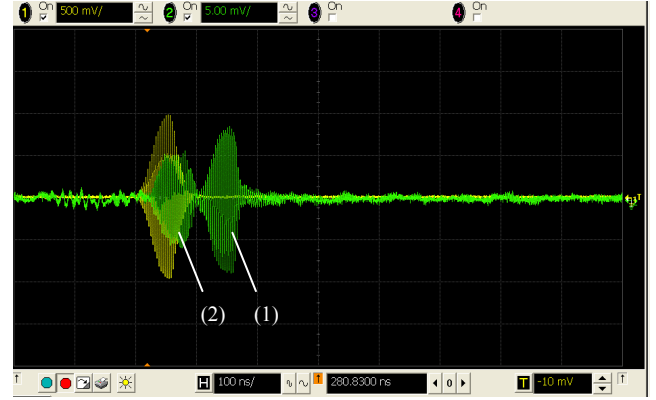


Fig. 5. Screen capture from the DSO80204B oscilloscope showing the time domain analysis of the superimposed transmitted (yellow) and received (green) 300 MHz 14 dBm signal modulated with a 80 ns square pulse, transmitted through the capacitively coupled cable. A ≈ 100 ns delayed transmitted pulse (1) is clearly visible, however part of the signal is now transmitted through radiation, as it is indicated by the radiated pulse (2).

C. Effects of CN Degradation

We have investigated the effects the degradation of the CNs has on the capacitive coupled GW. Figs. 6 and 7 show the transmitted (1) and radiated (2) pulses before and after a 5 inch gap was cut in all the CNs, respectively. The cut was made approximately 20 feet from the receiving funnel. One can clearly see an increase in the radiated pulse (2), and a decrease in the transmitted pulse (1). This indicated that some of the power is now radiated away at the CN break.

Next, we investigated the effects of the length of the gap on the signature of the transmitted pulse. Although still clearly present using a modulated pulse at 80 ns, the change is best visible when we increase the length of the modulated pulse to 100 ns. Fig. 8 and 9 shows the transmitted signal through a 5 inch and a 60 inch gap cut through all the CNs, respectively. Again, clearly visible is the decrease in size of the transmitted pulse (1), and the increase in size of the radiated pulse (2).

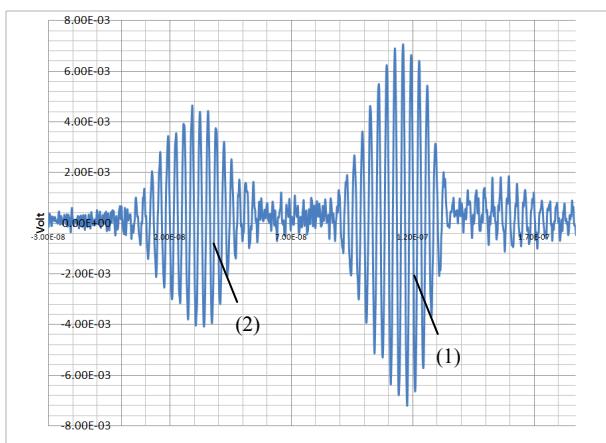


Fig. 6. The transmitted (1) and radiated (2) pulses (80 ns modulation) prior to the cut in the CNs.

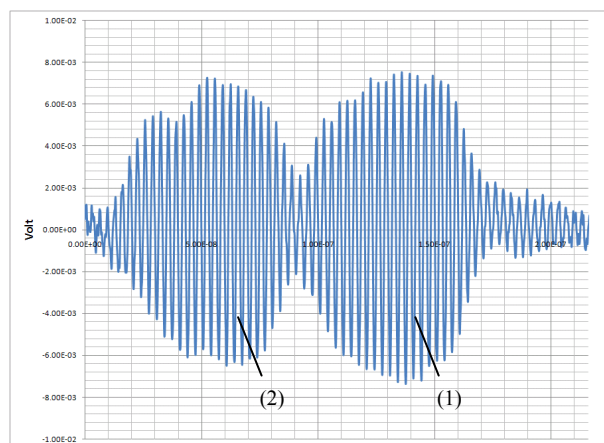


Fig. 8. The transmitted (1) and radiated (2) pulses (100 ns modulation) after a 5 inch cut was made in all the CNs.

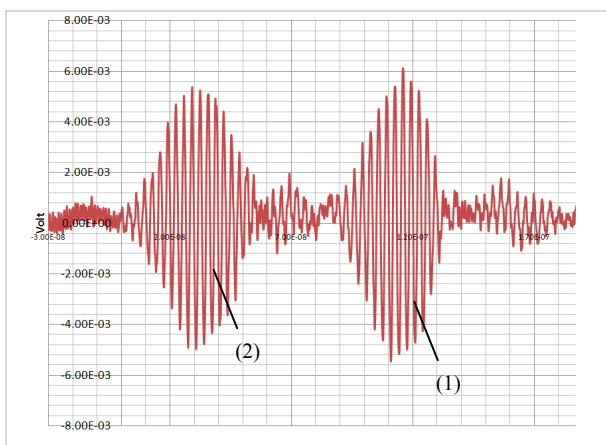


Fig. 7. The transmitted (1) and radiated (2) pulses (80 ns modulation) after a 5 inch cut was made in all the CNs.

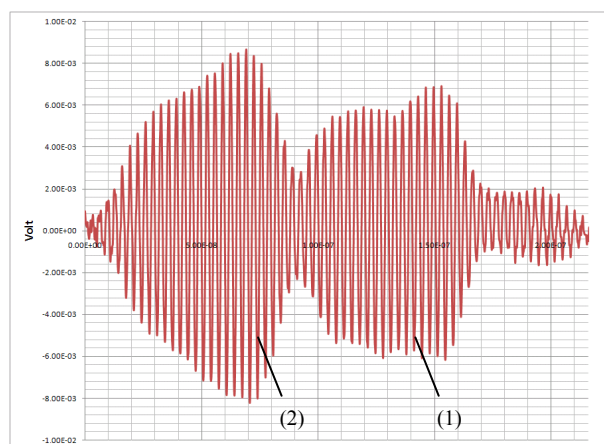


Fig. 9. The transmitted (1) and radiated (2) pulses (100 ns modulation) after the cut was enlarged to 60 inches.

VI. CONCLUSIONS

We are investigating the use of RF transmission lines as a method for probing the integrity of concentric neutrals in energized underground power distribution cables. We have looked at two approaches: the first approach couples a surface-guided RF wave (Goubau wave) to the concentric neutrals, while the second approach uses a two-wire transmission line between the adjacent concentric neutrals. Both approaches are applicable to probing the CN integrity without disconnecting and de-energizing the cable from the grid.

For this paper, we have concentrated on the application of the Goubau wave (GW), and have experimentally shown that a significant change occurs in the signature of the transmitted GW signal if the signal encounters a break in the CNs. Our data indicates that a gap in the concentric neutrals causes an increase in the amount of energy that is radiated away from the cable, thus changing the signature of the transmitted and received pulses in the time domain analysis. We are currently working on understanding the mechanism of the observed changes to the transmitted signal. We believe that such understanding will allow us to generalize the observed pattern to a set of markers that can then be employed to look for degraded spots in legacy underground power distribution cables.

We are also currently in the process of analyzing the information content of the reflected signal. Among other, we

are interesting in examining the effect of changes to the characteristic impedance between the CNs and the semicon, such as induced by a layer of corroded material, on the reflected (as well as transmitted) signal.

ACKNOWLEDGMENT

The authors of this paper would like to thank Walter Zenger, Tony Nothelfer and Al Valenzuela from PG&E, as well as John Erikson from Semptra Energy for providing us with many feet of underground distribution cable, terminations, and test equipment. We would also like to thank Steve Boggs, Tom Bialek and Jamie Patterson for their insightful comments and suggestions. This work was supported in part by the by grants from the California Energy Commission (CEC), contract numbers 500-02-004 and POB219-B.

REFERENCES

- [1] Goubau, G. "Surface Waves and Their Applications to Transmission Lines," J. App. Phys., Vol. 21, 1950.
- [2] Elmore, G. "Introduction to the Propagating Wave on a Single Conductor," Corridor Systems Inc., July 7th 2009.
- [3] Stratton, J.A. "Electromagnetic Theory." McGraw-Hill Book Company, 1st ed., 1941.

AMR Current Sensors for Evaluating the Integrity of Concentric Neutrals in In-Service Underground Power Distribution Cables

Michael Seidel

Dept. of Mechanical Engineering
University of California
Berkeley, CA, 94720, USA
mjseidel@berkeley.edu

Kanna Krishnan

Berkeley Sensor and Actuator Center
University of California
Berkeley, CA, 94720, USA
kannak@berkeley.edu

Igor Paprotny

Berkeley Sensor and Actuator Center
University of California
Berkeley, CA, 94720, USA
igorppapa@eecs.berkeley.edu

Richard White

Berkeley Sensor and Actuator Center
University of California
Berkeley, CA, 94720, USA
rwhite@eecs.berkeley.edu

James Evans

Dept. of Materials Science and Engineering
University of California
Berkeley, CA, 94720, USA

In this paper, we present a new method to diagnose the integrity of concentric neutral wires in underground power distribution cables. This method uses a commercially available 3-axis anisotropic magnetoresistive (AMR) magnetic field sensor chip. The AMR sensor is passed once along the energized cable axially, and the cable's 3-axis magnetic field is plotted as a function of position over the cable. Peaks corresponding to the individual concentric neutral currents are observed, and can be analyzed to diagnose breaks in concentric neutrals due to total corrosion or other means.

***Keywords:* concentric neutrals, underground power distribution cables, AMR sensors, cable diagnostics, in service, magnetic current sensing**

I. INTRODUCTION

The failures of underground power distribution cables represent a serious threat to the reliability of power infrastructure. Underground distribution cables operate under adverse conditions, being subjected to daily and seasonal thermal cycles as well as submersion in electrolyte-bearing groundwater, and are thus expected to degrade over time. However, current underground cable diagnostic techniques require the cable to be disconnected from the grid to perform the diagnostic. Therefore, there is a need for an effective diagnostic method that can be applied to the cable without disconnecting them from the grid. With such a diagnostic, utilities could replace cables selectively according to their

diagnosed condition, resulting in fewer costly failures that interrupt service to the consumer. Our goal is to develop a technique to assess the condition of concentric neutral wires (CNs) on underground power distribution cables that fulfills two requirements: First, that the method can be used while the cable under test is in service, avoiding the expense associated with de-energizing a cable to test it; second, that the method is suitable for use on jacketed cables as well as unjacketed "direct-buried" cables.

Currently, the primary methods of cable testing are tan-delta measurements [1] and time-domain reflectometry methods [2,3]. Of these, only the latter is suitable for detection of CN degradation, and it requires that the cable be de-energized for testing.

In this paper, we propose a method for diagnosing the health of CNs in underground power distribution cables using a 3-axis magnetic field sensor placed in close proximity or contact with the outside of the cable, and either moved along the cable in the axial direction, or rotated around the cable. From this magnetic field information the currents in the individual concentric neutrals can be determined with enough accuracy to predict their intact or broken condition.

II. MODELING

The magnetic fields outside of a cable due to currents in the

This work was supported in part by the by grants from the California Energy Commission (CEC) - contract numbers 500-02-004 and POB219-B

center conductor and CNs were modeled using MATLAB; the results of this modeling are shown in Figs. 1-4. A simplified two-dimensional model was used. In this model, the CNs were treated as straight wires distributed evenly around the center conductor of a two-inch cable containing twelve concentric neutrals. Calculations of the magnetic field at the simulated sensor location were carried out by use of the Biot-Savart law. To simulate the axial movement of the sensor which occurs during experiment, the sensor was modeled to rotate around the circumference of the two-dimensional model. In all simulations, the current in the CNs was set to be 3A RMS in total.

Two cases of center conductor current were considered: That of no current, and that of 3A RMS in the direction opposite to the concentric neutral current. Each of these cases was simulated once with all intact CNs, and once with a single CN missing.

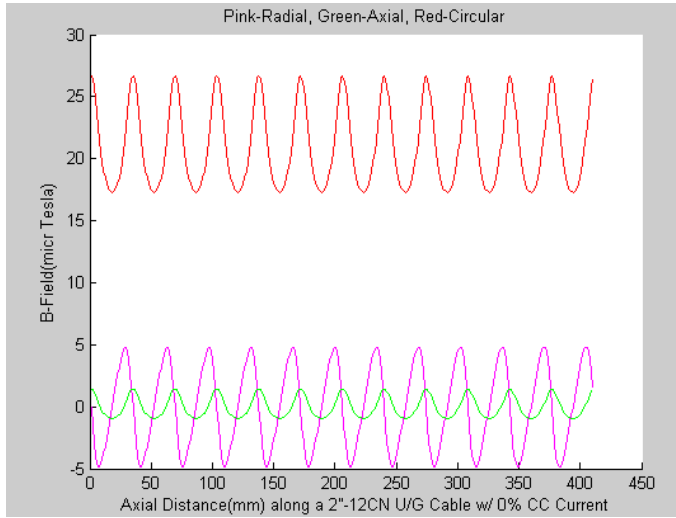


Fig. 1. 0% center conductor (CC) current.

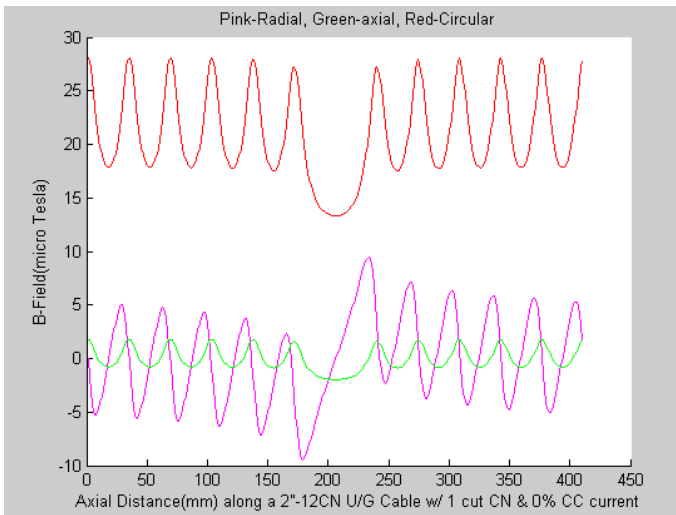


Fig. 2. 0% center conductor (CC) current, one broken concentric neutral (CN).

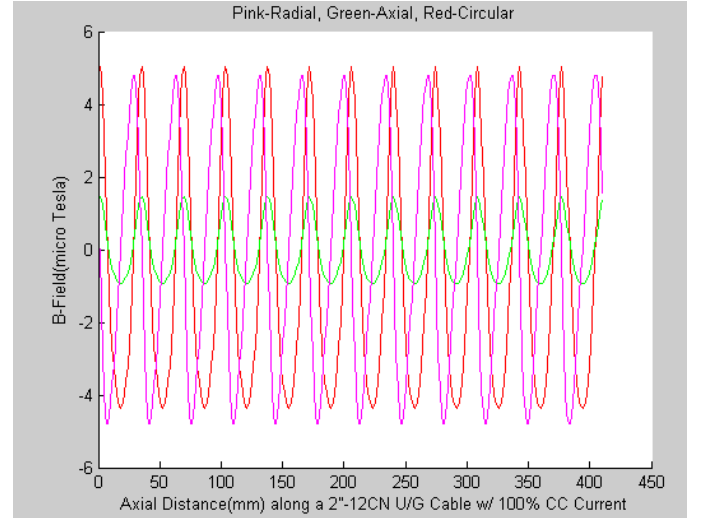


Fig. 3. 100% center conductor (CC) current.

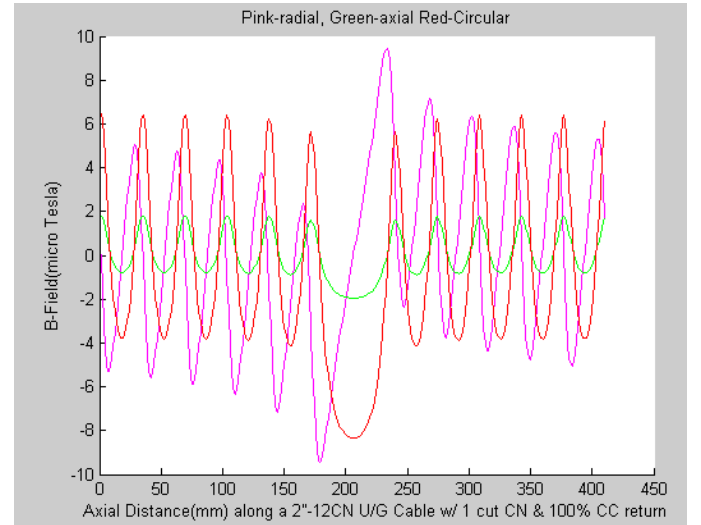


Fig. 4. 100% center conductor (CC) current, one broken concentric neutral (CN).

III. EXPERIMENTAL RESULTS

A. Experimental Setup

The experiments were performed on a section of two-inch diameter, jacketed, XLPE-insulated cable. Two variable transformers driven by 60Hz line voltage were used to drive currents in the central conductor and concentric neutrals, respectively. In each experiment, 3A RMS was driven through all the concentric neutrals, and a fraction of the current was driven through the center conductor. A one ohm current-balancing load resistor was placed in series with each concentric neutral at the termination of the cable to ensure an

even distribution of current among the unbroken concentric neutrals.

The same length of cable was used for those experiments in which a concentric neutral was treated as broken. To simulate this break, one of the one-ohm balancing resistors was removed from the circuit, leaving the corresponding concentric neutral carrying zero current.

An anisotropic magneto-resistive (AMR) sensor used is the HMC1043 device, manufactured by Honeywell. This device is three millimeters square, and thus possesses good spatial resolution to distinguish between the currents in separate concentric neutrals. The device was provided by Honeywell soldered to a one inch square PCB with onboard amplifier. The device was powered by an Agilent E3631A DC power supply. Because the AMR device needs periodic set/reset pulses to function correctly, an Agilent 33220A function generator was used to provide a set/reset pulse to the device every four minutes. The AMR sensor was passed down the axial length of the cable and the three-axis values of magnetic field on the surface of the cable jacket recorded. The total length of travel was slightly longer than that required to pass above one concentric neutral twice. The AMR sensor was moved with a metric lead screw assembly for this experiment, but consideration has been given to deployable measurement techniques. These considerations are discussed in section IV.

B. Results

Figs. 5 - 8 depict the three axes of magnetic field outside the experimental cable for one ratio of current (center conductor to concentric neutral) and one condition of the experimental concentric neutral (broken or unbroken). Lines connecting the data points have been added for clarity, given that each plot contains three multiply-intersecting curves. Note that the magnetic field values are RMS values, yet they swing positively and negatively; our convention is to plot the magnitude of the RMS value as positive or negative to indicate the phase of the 60Hz B-field waveform at that point as referenced against the line voltage. Thus, these curves indicate the phase of the magnetic field waveform as well as RMS magnitude of the magnetic field.

Apparent in the curves is a series of peaks, each corresponding to sensor location being directly above a current-carrying concentric neutral. In the two sets of curves for which a concentric neutral was broken, a characteristic disturbance can be seen: In the axial and circumferential fields this disturbance appears as a local minimum where a current peak would appear in a healthy cable, as predicted by modeling. In the radial field, this disturbance appears as a swing between phases and between two peaks, similarly to that predicted by modeling. These qualitative attributes of the magnetic field may be sufficient for the diagnosis of broken concentric neutrals by a trained technician in the field; such qualitative assessment is routinely used by technicians to detect cable insulation defects in partial discharge tests.

Further modeling and experiments are underway to algorithmically determine concentric neutral condition from measured magnetic field data.

IV. DEPLOYMENT CONSIDERATIONS

In the field, magnetic field scans of underground distribution cables can be performed by utility technicians equipped with *hotsticks*, which are insulated rods used for manipulation of high-voltage equipment. The underground distribution cable can be accessed at their ends in vaults. We envision a commercial apparatus that can be affixed to a hotstick and pushed by a technician along a cable, possessing the following: One or more AMR sensors, a mechanical means of ensuring a reasonably constant distance between the sensors and the cable, a mechanical means of ensuring a reasonably constant radial orientation of the sensors on the cable, a wireless sensor node to sample data from the sensors and store it or transmit it to a data storage device, and a wheel pressed into contact with the cable jacket and connected to an optical encoder or potentiometer to record the relative position of the apparatus to the cable at each AMR data sample.

We have constructed a prototype of such a device, with the exception of the integrated wireless sensor node, using a ten-turn potentiometer as the position-tracking element. The mechanical guide ensuring fairly constant distance between sensor and cable is a piece of HDPE with a one-inch diameter semicircular bore in it.

We have considered that some cable vaults may give access to only short lengths of cable, and that in any case such hotstick manipulation as described above may prove difficult to perform repeatably; for these reasons we have considered an alternative deployment method for magnetic sensors: A device which is placed around a cable like a bracelet, and is either rotated around the cable to measure the currents in each concentric neutral, or which possesses a sufficient distribution of multiple sensors to adequately assess concentric neutral condition while stationary. Such a cable “bracelet” is depicted in Fig. 9.

Modeling work is underway to assess the number of sensors and/or degrees of rotation about a cable necessary to assess concentric neutral condition with such a device.

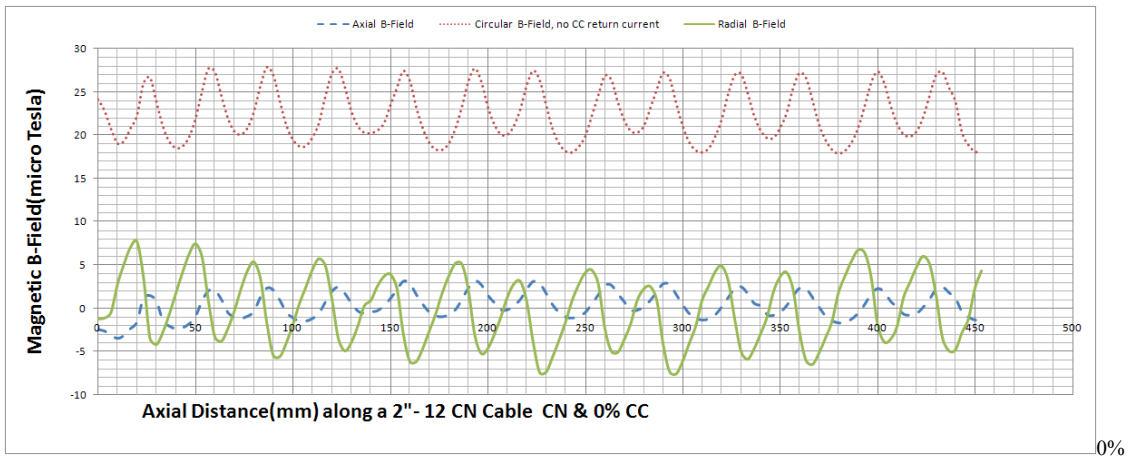


Fig. 5. 0% center conductor (CC) current.

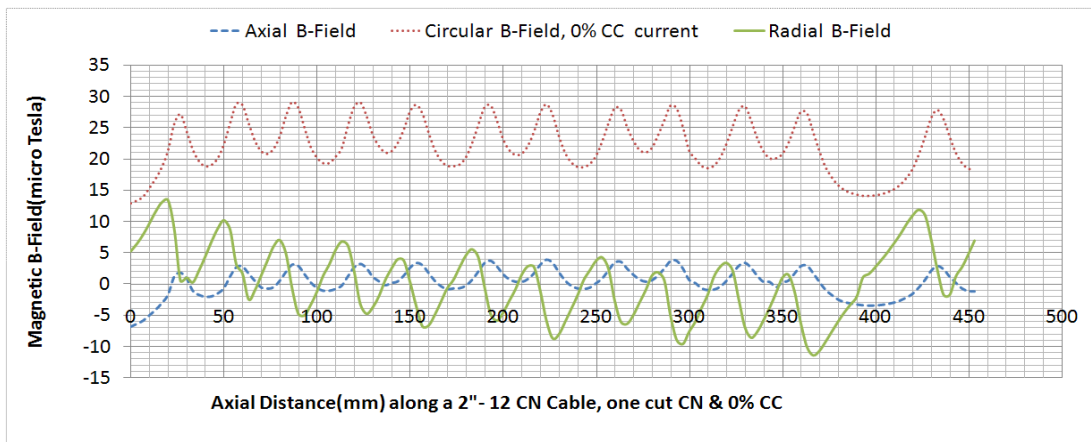


Fig. 6. 0% center conductor (CC) current, one broken concentric neutral (CN)

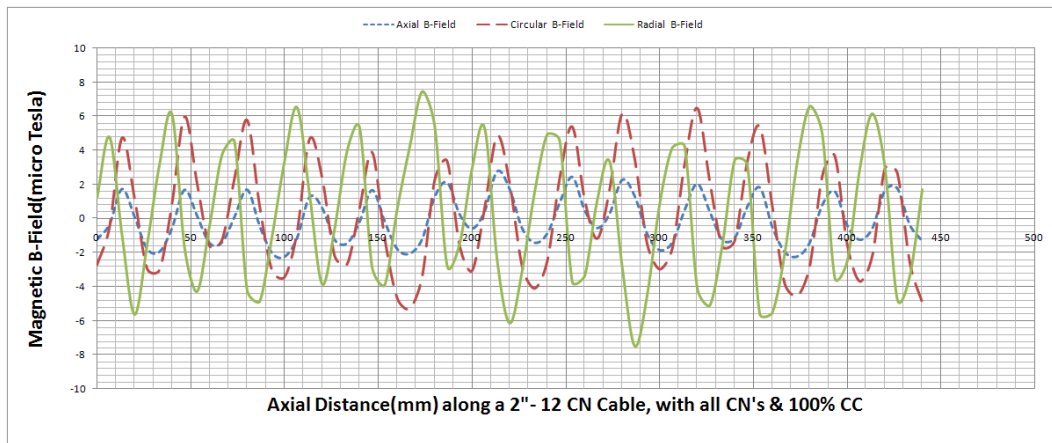


Fig. 7. 100% center conductor (CC) current.

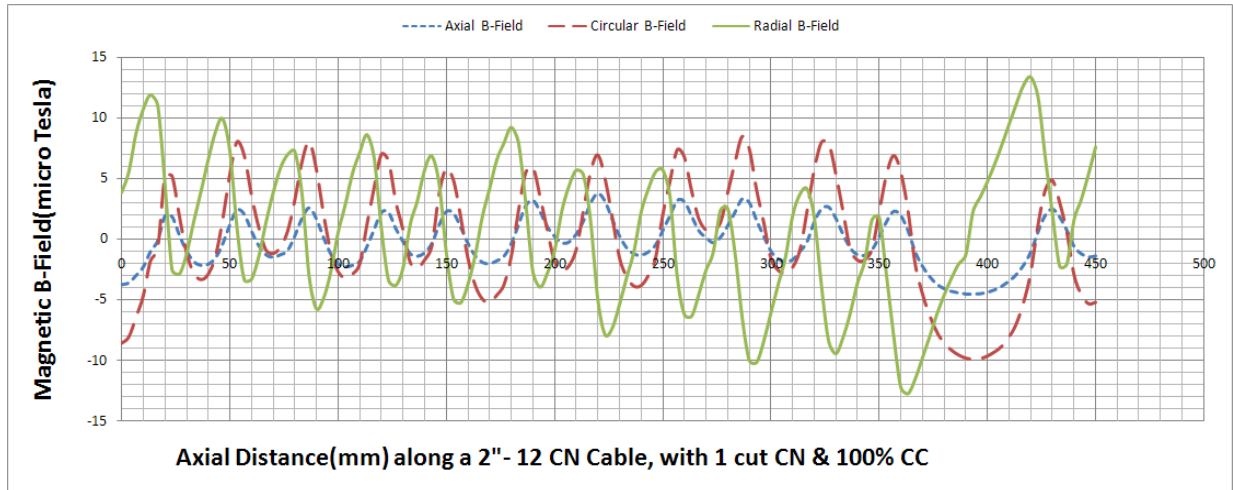


Fig. 8. 100% center conductor (CC) current, one broken concentric neutral (CN).

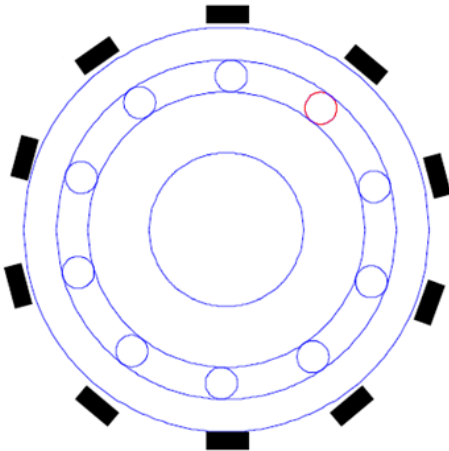


Fig. 9. Cross-section of cable with AMR sensors (shown in black) encircling cable under test.

ACKNOWLEDGMENT

The authors of this paper would like to thank Walter Zenger, Tony Nothelfer and Al Valenzuela from PG&E, as well as John Erikson from Semptra Energy for providing us with many feet of underground distribution cable, terminations, and test equipment. We would also like to thank Steve Boggs, Tom Bialek and Jamie Patterson for their insightful comments and suggestions. This work was supported by grants from the California Energy Commission (CEC), contract numbers 500-02-004 and POB219-B, as well as research and infrastructural grants from the Berkeley Sensor & Actuator Center (BSAC) and the Center for Information Technology Research in the Interest of Society (CITRIS), at UC Berkeley.

REFERENCES

- [1] A. Ponnirani and M.S. Kamarudin, "Study on the performance of underground XLPE cables in service based on tan delta and capacitance measurements," *IEEE 2nd Annual Power and Energy Conference*, pp. 39-43, Dec. 2008.
 - [2] R. Papazyan and R. Eriksson, "High frequency characterisation of water-treed XLPE cables," *Proceedings of the 7th International Conference on Properties and Applications of Dielectric Materials*, pp. 187-190, June 2003.
- "IEEE Guide for Detection, Mitigation, and Control of Concentric Neutral Corrosion in Medium-Voltage Underground Cables," *IEEE Std 1617-2007*, Feb. 18 2007